Pharmacological Research xxx (2017) xxx–xxx

Contents lists available at ScienceDirect

Pharmacological Research

journal homepage: www.elsevier.com/locate/yphrs

Perspective

ES2 enhances the efficacy of chemotherapeutic agents in ABCB1-overexpressing cancer cells *in vitro* and *in vivo*

Yanfen Fang[a,b,1], Juanjuan Sun[a,c,1], Xing Zhong[a,1], Rui Hu[d], Jie Gao[d], Guanfu Duan[a], Changge Ji[a], Lijuan Chen[a], Wanli Zhang[a], Chunxiao Miao[a], Haji Akber Aisa[d,*], Xiongwen Zhang[a,*]

[a] *Shanghai Engineering Research Center of Molecular Therapeutics and New Drug Development, School of Chemistry and Molecular Engineering, East China Normal University, Shanghai, China*
[b] *Division of Anti-Tumor Pharmacology, Shanghai Institute of Materia Medica, Chinese Academy of Sciences, Shanghai, China*
[c] *State Key Laboratory of Cell Biology, Center of Excellence in Molecular and Cell Biology, Shanghai Institute of Biochemistry and Cell Biology, Chinese Academy of Sciences, Shanghai, China*
[d] *The Key Laboratory of Plant Resources and Chemistry of Arid Zone, Xinjiang Technical Institute of Physics and Chemistry, Chinese Academy of Sciences, Urumqi, China*

ARTICLE INFO

Article history:
Received 4 August 2017
Received in revised form 26 October 2017
Accepted 2 November 2017
Available online xxx

Keywords:
MDR
ABCB1
Jatrophane diterpenoid ester
Chemotherapeutic agents

ABSTRACT

ES2 is a new type of jatrophane diterpenoid ester isolated from the fructus E. *sororia*, a traditional Uyghur medicine in China. Here we reported the multidrug resistance (MDR) reversal effect of ES2 *in vitro* and *in vivo* by modulating the function of ATP-binding cassette subfamily B member 1 (ABCB1). ES2 exhibited low cytotoxicity to ABCB1-overexpressing MDR cells and their parental sensitive cells, but sensitized the MDR cells and ABCB1-transfected HEK293 cells to chemotherapeutic drugs that are ABCB1 substrates. The reversal ability of ES2 was primarily due to the inhibition of the efflux function of ABCB1. Moreover, ES2 stimulated the ATPase activity of ABCB1 in a concentration-dependent manner. There was no change in the expression of ABCB1 in the presence of ES2. The molecular docking analysis indicated that ES2 bond to the drug-binding site of ABCB1 transporter. Importantly, ES2 significantly enhanced the anti-tumor effect of vinorelbine against KBv200 cell xenografts in nude mice. Overall, these findings demonstrate that ES2 inhibits the ABCB1 transporter function and consequently reverses ABCB1-mediated MDR, indicating the potential use of ES2 in combination therapy with conventional chemotherapeutic drugs for cancer treatment.

1. Introduction

Multidrug resistance (MDR), the ability of cancer cells to acquire drug resistance to a broad spectrum of anticancer drugs that are structurally and functionally unrelated, remains one of the major reasons for the clinical failure of cancer chemotherapy [1–3]. Of the potential mechanisms that mediate the development of MDR, the most predominantly reported ones are those which associate with the overexpression of various members of the ATP binding cassette (ABC) transport proteins. By actively pumping the chemotherapeutic drugs out of the cancer cells, these ABC transporters decrease the intracellular drug accumulation, therefore causing drug resistance [2–5].

The human ABCB1/MDR1/*P*-glycoprotein (P-gp), a classical and the best-studied ABC transporter, is usually significantly augmented in drug-resistant tumor [6–8]. ABCB1 can extrude out multiple types of chemotherapeutic drugs, including vinca alkaloids (vincristine, vinblastine), taxanes (paclitaxel, docetaxel), anthracyclines (doxorubicin, epirubicin) and epipodophyllotoxins (etoposide) [8]. Inhibiting the function of ABCB1 or decreasing its expression could effectively increase the intracellular accumulation and anti-cancer effects of these drugs on MDR cancer cells. To date, three generations of ABCB1 inhibitors have been developed. However, the outcomes from clinical trials were not ideal, which were highly correlated with unacceptable side effects and unexpected drug–drug interactions [4]. Therefore, developing or

Abbreviations: MDR, multidrug resistance; ABCB1, ATP-binding cassette subfamily B member 1; ABC, ATP binding cassette; P-gp, P-glycoprotein; Rho123, rhodamine-123; NVB, Vinorelbine; PTX, paclitaxel; DOX, doxorubicin; DDP, cisplatin; TPT, topotecan; VPL, Verapamil; FTC, Fumitremorgin C; RLU, relative light units; RTV, relative tumor volume; TGI, tumor growth inhibition.

* Corresponding authors.
E-mail addresses: haji@ms.xjb.ac.cn (H.A. Aisa), xwzhang@sat.ecnu.edu.cn (X. Zhang).

[1] These authors contributed equally to this work.

https://doi.org/10.1016/j.phrs.2017.11.001
1043-6618/

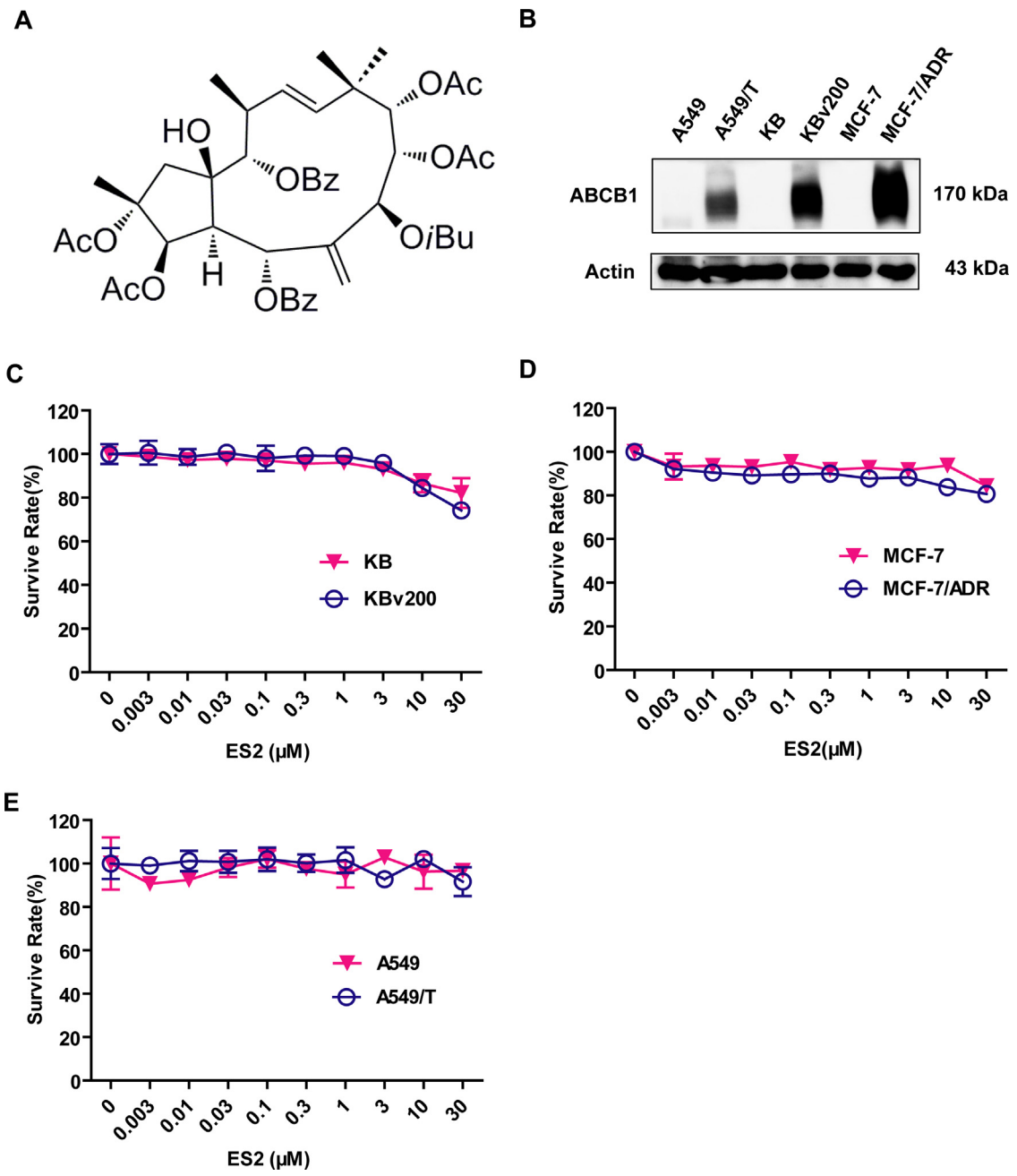

Fig. 1. ES2 exhibits low cytotoxicity to drug resistant cell lines and parental cell lines. (A) Structure of ES2. (B) The protein expression of ABCB1. (C–E) Cells were treated with the indicated concentration of ES2 for 72 h, and cell survival was measured by MTT assay. Each point represents the mean ± SD from the cells of triplicate wells. The experiments were repeated three times.

searching for novel ABCB1 inhibitors with higher efficacy and lower toxicity still requires plenty of works.

Natural active constituents isolated from plants, usually with the properties of lower toxicity and fewer side effect, have been becoming important resources to obtain novel MDR modulators. For example, flavonoids, tetrandrine, and emodin have been reported for their effects on reversing ABCB1-mediated MDR [9–12]. *Euphorbia sororia* A. Schrenk, an annual herb, is mainly distributed in northwest China and in some middle Asia countries. The fructus E. *sororia* is a traditional Uyghur medicine in China and has been used to treat abdominal distention, abdominal pain, skin disease and paralysis [13,14]. We have previously isolated a new type of Jatrophane diterpenoid ester, ES2 (Fig. 1A) from the fructus E. *sororia* and found it increased the intracellular accumulation of rhodamine-123 (Rho123) in ABCB1-overexpessing cell lines, indicating the potential ABCB1 inhibition effect of ES2 [15]. However, to what extent ES2 inhibits P-gp function and whether this activity contributes to MDR reversal remains unknown. This study has been focused on systematically investigating the MDR reversal activity of ES2 *in vitro* and *in vivo*, and elucidating its underlying mechanisms.

2. Materials and methods

2.1. Chemicals

ES2 was isolated from the acetone extract of fructus *Euphorbia sororia* by Prof. Haji Akber Aisa of Xinjiang Technical Institute of Physics and Chemistry. MTT, Vinorelbine (NVB), Paclitaxel (PTX),

Please cite this article in press as: Y. Fang, et al., ES2 enhances the efficacy of chemotherapeutic agents in ABCB1-overexpressing cancer cells *in vitro* and *in vivo*, Pharmacol Res (2017), https://doi.org/10.1016/j.phrs.2017.11.001

Cisplatin (DDP), Topotecan (TPT), Verapamil (VPL), Fumitremorgin C (FTC) and Rho123 were purchased from Sigma-Aldrich. Doxorubicin (DOX) and MK571 were from Selleck. For *in vitro* assays, ES2, NVB, PTX, DOX, DDP and TPT were dissolved in DMSO as 100 mM stock solution; for *in vivo* studies, ES2 was suspended in 0.5% carboxumethyl cellulose and 5% DMSO and NVB was dissolved in physiological saline.

2.2. Cell lines and cell culture

Human oral epidermoid carcinoma cell line KB and its vincristine-selected derivative ABCB1-overexpressing cell line KBv200, DOX-selected ABCB1-overexpressing breast carcinoma cell line MCF-7/ADR and Paclitaxel-selected ABCB1-overexpressing lung carcinoma cell lines A549/T were generously provided by Liguang Lou (Shanghai Institute of Materia Medica, Chinese Academy of Sciences). MCF-7 and A549 cells were obtained from American Type Culture Collection (ATCC). Stable-transfected HEK293/pBABE, HEK293/ABCB1, HEK293/ABCG2 and HEK293/ABCC1 cells were established by selection with puromycin (Genomeditech, Shanghai, China) after transfecting HEK293 with empty pBABE or pBABE vector containing full-length of ABCB1, ABCG2 or ABCC1, respectively. All cells were cultured in essential medium containing 10% FBS at 37 °C in a humidified atmosphere of 5% CO2.

2.3. Cell cytotoxicity test

MTT assay was carried out to assess the sensitivity of cells to chemotherapeutic drugs [16]. Briefly, cells were plated in 96-well plates and allowed to attach overnight, and then various concentrations of ES2 and/or a full range concentration of conventional chemotherapeutic drug (NVB, PTX, DOX and DDP) were added to the wells. After 72 h of incubation, MTT (0.5 mg/mL) was added into each well and incubated for an additional 1 h or 4 h (37 °C). Subsequently, the medium was discarded, and 100 μL of DMSO was added to dissolve the formazan product from the metabolism of MTT. The optical density was measured at 550 nm using a microplate reader (SpectraMax M5 Multi-Mode Microplate Readers, Molecular Devices). The concentration required to inhibit cell growth by 50% (IC_{50}) was calculated from survival curves using GraphPad Prism 5.0 software. The degree of resistance was estimated by dividing the IC_{50} for the MDR cells by that of the parental sensitive cells. The fold-reversals were calculated as IC_{50} for cells with the anticancer drug in the absence of inhibitors divided by that in the presence of inhibitors.

2.4. Fluorescence microscope observation of intracellular DOX and Rho123

KB and KBv200 cells were seeded in 96-well plates and allowed to attach overnight. The cells were pretreated with various concentrations of ES2 (0, 1, 10 μM) or VPL (10 μM) for 4 h at 37 °C and then treated with DOX (10 μM) or Rho123 (10 μM) for an additional 1 h in darkness at 37 °C. After washed twice with ice-cold PBS, cell images were captured by a fluorescence microscopy (Olympus IX3).

2.5. Flow cytometric analysis of the accumulation of Rho123

The effect of ES2 on the cellular accumulations of Rho 123 or DOX was measured by flow cytometry as previously described with some modifications [17]. Cells were seeded in 6-well plates and allowed to attach overnight and then incubated with various concentrations of ES2 (0, 0.1, 0.3, 1, 3, 10 μM) or VPL (10 μM) at 37 °C for 4 h. Cells were then treated with Rho123 (10 μM) or DOX (10 μM) for an additional 1 h in darkness at 37 °C. Following this incubation, cells were collected and analyzed by flow cytometry (Guava EasyCyte 6HT2L). At least 10,000 cells per samples were counted and acquired. The relative values were identified by dividing the fluorescence intensity of each measurement by that of control cells.

2.6. Flow cytometric analysis of Rho123 efflux

Rho123 efflux was determined following a modification of methods described earlier [17,18]. Briefly, KB and KBv200 cells were incubated with Rho123 (10 μM) for 1 h at 37 °C. Cells were washed with PBS and then incubated in Rho123-free medium with or without 10 μM ES2. Subsequently, at 0, 15, 30, 60, 90 and 120 min, cells were collected for flow cytometric analysis. At least 10,000 cells per samples were counted and acquired.

2.7. ABCB1 ATPase activity assay

The changes of ATPase activity were evaluated by ABCB1-Glo™ assay systems (Promega Corp., Madison, WI, USA). Sodium orthovanadate (Na_3VO_4) was used as a selective inhibitor of ABCB1 ATPase. For the impact of ES2 on ABCB1 ATPase activity, ABCB1-Glo™ Assay Buffer, Na_3VO_4 (0.25 mM), VPL (0.5 mM) or ES2 at various concentrations, recombinant human ABCB1 membranes (25 μg) and MgATP (25 mM) were added into designated white opaque 96-well plate in turn. For the impact of ES2 on verapamil-stimulated ABCB1 ATPase activity, ABCB1-Glo™ Assay Buffer, Na_3VO_4 (0.25 mM), VPL (0.5 mM), ES2 at various concentrations, recombinant human ABCB1 membranes (25 μg) and MgATP (25 mM) were added into designated white opaque 96-well plate in turn. And then the plate was incubated at 37 °C for 80 min. Subsequently, luminescence was initiated by ATP detection buffer. After incubation at room temperature for 20 min to allow luminescent signal to develop, the plate was read on a luminometer (spectraMax M5, molecular devices, USA). The relative light units (RLU) in the untreated samples (NT) compared to the Na_3VO_4-treated samples reflects the consumption of ATP by the basal P-gp ATPase activity. The RLU in the ES2 or/and VPL-treated samples compared to the Na_3VO_4-treated samples reflect the consumption of ATP by compounds. The results were represented by comparing the ATP consumption in the compound treated samples to the basal ATP consumption.

2.8. Real-time quantitative PCR

After treating the KBv200 cells with different concentrations and for different duration of ES2, total cellular RNA was isolated by Trizol Reagent (Invitrogen, Carlsbad, CA, USA) following manufacturer's instruction. The first strand cDNA synthesis and amplification were performed according to the M-MLV 1 st Strand Kit protocol (Invitrogen, Carlsbad, CA, USA). Real-time PCR was performed as described in the SYBR premix Ex Taq protocol (Takara) with a CFX96 Real-Time PCR platform (BIO-RAD). Specific PCR primers used were 5′-GTGGGGCAAGTCAGTTCATT-3′ (forward) and 5′-TCTTCACCTCCAGGCTCAGT-3′ (reverse) for ABCB1 [19] and 5′-CTGCACCACCAACTGCTTAG-3′ (forward) and 5′-TTCAGCTCAGGGATGACCTT-3′ (reverse) for GAPDH [20]. GAPDH mRNA levels were used for normalization. The fold-change for gene expression was calculated using the Pfaffl method.

2.9. Western blot

Cells after different treatment were lysed with RIPA Lysis and Extraction Buffer (Thermo) containing protease and phosphatase inhibitor cocktail (100×) (Thermo scientific). The protein concentration was determined using a BCA assay (Beyotime

Please cite this article in press as: Y. Fang, et al., ES2 enhances the efficacy of chemotherapeutic agents in ABCB1-overexpressing cancer cells *in vitro* and *in vivo*, Pharmacol Res (2017), https://doi.org/10.1016/j.phrs.2017.11.001

Biotechnology, Haimen, China) and equalized before loading. A total of 10–40 μg of protein extracted from cultured cells was separated by 6%-10% SDS-PAGE and transferred onto PVDF membranes. After the membranes were blocked and blotted with the relevant primary antibodies, the membranes were then incubated with HRP-conjugated secondary antibody, and then visualized using the WB Femto ECL Substrate (Thermo scientific). The expression of GAPDH or Actin was used as loading control. Primary antibodies used were as follows: ABCB1 (P7965) Sigma-Aldrich (St. Louis, MO); ABCC1 (ab32574) (abcam, Cambridge, UK); ABCG2 (4477) (Cell Signaling technology, Inc, Beverly, MA); and Actin (sc-1615) (Santa Cruz Biotechnology, Dallas, TX).

2.10. Molecular modeling of ABCB1

The crystal structures of mouse ABCB1 in complex with QZ59-RRR (PDB ID: 4M2S) and QZ59-SSS (PDB ID: 4M2T) were used to generate the drug-bound homology model of the human ABCB1 as previously described [21]. Homology models were generated by SWISS-MODEL (http://swissmodel.expasy.org/). The 3D structures of ES2 and VPL were built using the fragment dictionary of Maestro v10.1. Docking simulations of ES2 and VPL were carried out using the "Extra precision" (XP) mode of Glide docking program version6.5 (Schrödinger, LLC, New York, NY, 2014) and the parameters were by default in this software. The top-scoring pose-ABCB1 complex structures were used for graphical analysis.

2.11. Nude mice xenograft tumor assay

Female BALB/c nu/nu mice (5–6 weeks, 16–18 g) were obtained from Sino-British SIPPR/BK Lab. Animal Ltd, Shanghai, China, with the certification number of 2008001638201. The animals were housed in specific pathogen-free (SPF) conditions at Key Laboratory of Brain Functional Genomics, Ministry of Education, East China Normal University, and were acclimatized for a week prior to use. The use and care of experimental animal was approved by Institutional Animal Care and Use Committee, East China Normal University.

Human KBV200 xenografts were established by subcutaneously inoculating 3×10^6 cells into the right armpit of athymic nude mice (BALB/C-nu/nu, female). When the tumors reached a mean group size of $100 \sim 150\,mm^3$, the mice were randomized into four groups and received various treatments: (i) vehicle (q3d); (ii) NVB (4 mg/kg, intraperitoneal injection/i.p., q3d); (iii) ES2 (150 mg/kg, gavage/p.o, q3d); (iv) NVB (4 mg/kg, intraperitoneal injection/i.p., q3d) plus ES2 (150 mg/kg, gavage/p.o, q3d). The tumor growth was recorded with the measurement of length (L) and width (W) by caliper three times a week, and calculated as tumor volume $(V) = L \times W^2/2$. The relative tumor volume (RTV) on day n was calculated according to the following formula: $RTV = TV_n/TV_0$, where TV_n is the tumor volume on day n and TV_0 is the tumor volume on day 0. The tumor growth inhibition was calculated as TGI% = (1 − (mean tumor volume of the treatment group on the first day-mean tumor volume of the treatment group on the end day)/(mean tumor volume of the control group on the first day-mean tumor volume of the control group on the end day)) × 100%.

2.12. Color figures preparation

Color figures were prepared following the published guidelines [22].

2.13. Statistical analysis

The statistical significance of differences between groups was evaluated by the unpaired Student's t-test and indicated with $^{***}P < 0.001$, $^{**}P < 0.01$, $^{*}P < 0.05$. All statistical tests were two sided.

3. Results

3.1. Anti-proliferative effects of ES2 on ABCB1-overexpessing cancer cell lines and their parental cells

To characterize ABCB1-overexpressing and corresponding parental cell lines, we first detected ABCB1 expression by Western blot in three pairs of cell lines. As shown in Fig. 1B, ABCB1 was overexpressed in KBv200, MCF-7/ADR and A549/T cell lines, while was almost undetectable in their respective parental cell lines. MTT assay was then performed to determine the anti-proliferative effect of ES2 alone on these cell lines. The results showed that ES2, at up to 30 μM, exhibited weak anti-proliferative effects on both ABCB1-overexpressing cells and their parental sensitive cells. Notably, more than 85% of cells survived after treated with ES2 at the concentration of 10 μM for 72 h (Fig. 1C–E). Therefore, ES2 at a maximum concentration of 10 μM was used in the following experiments to determine its MDR reversal activity and to investigate underlying mechanisms.

3.2. ES2 sensitizes ABCB1-overexpressing cells to chemotherapeutic agents

To determine whether ES2 could reverse ABCB1-mediated MDR, cell survival assay was performed in the presence or absence of a range of different concentration of ES2 (0.1, 0.3, 1, 3, 10 μM), using ABCB1-overexpressing cells (KBv200 and MCF-7/ADR) and their parental cells (KB and MCF-7). A control ABCB1 inhibitor (VPL, 10 μM) was used for comparison. As expected, two MDR cell lines were highly resistant to NVB, PTX or DOX (all are substrates of ABCB1) than their parental cell lines. In the presence of ES2, both the MDR cell lines, but not their parental cells, were found to be sensitized to these chemotherapeutic agents (Figs. 2 and 3). And the MDR reversal activity of ES2 was in a dose-dependent manner. The IC_{50} values of anti-cancer drugs (NVB, PTX and DOX) in all cell lines were shown in Tables 1 and 2. Of note, the reversal effect of ES2 was more potent than verapamil at the same concentration in both cell lines. For example, in KBv200 cells, treatment with 10 μM ES2 reduced the IC_{50} of NVB by 315.44-fold and PTX by 82.54-fold, respectively; however, treatment with 10 μM verapamil only reduced the IC_{50} of NVB by 43.88-fold and PTX by 26.25-fold, respectively. In addition, ES2 did not alter the cytotoxicity of DDP which is not an ABCB1 substrate either in MDR cells or their parental sensitive cells.

3.3. ES2 does not enhance the sensibility of ABCG2- or ABCC1-overexpressing cells to chemotherapeutic agents

In order to determine the effects of ES2 on ABCG2-or ABCC1-mediated MDR, we established HEK293/ABCB1, HEK293/ABCG2 and HEK293/ABCC1 cells. Overexpression of ABCB1, ABCG2 and ABCC1 in HEK293 cells and drug resistance to their respective substrates were shown in Supplemental Fig. S1. The 10 μM was chosen as a non-toxic concentration for ES2, because more than 90% of these cells survived at 10 μM (Fig. 4A–C). As expected, ES2 successfully sensitized HEK293/ABCB1 cells to DOX without altering the sensitivity of HEK293/pBABE cells (Fig. 4A and Table 3). However, ES2 could not alter the sensitivity of HEK293/pBABE and HEK293/ABCG2 cells to TPT while FTC, a positive inhibitor of ABCG2, was able to reverse the resistance of HEK293/ABCG2 to TPT (Fig. 4B and Table 3). In addition, ES2 slightly decreased the resistance of

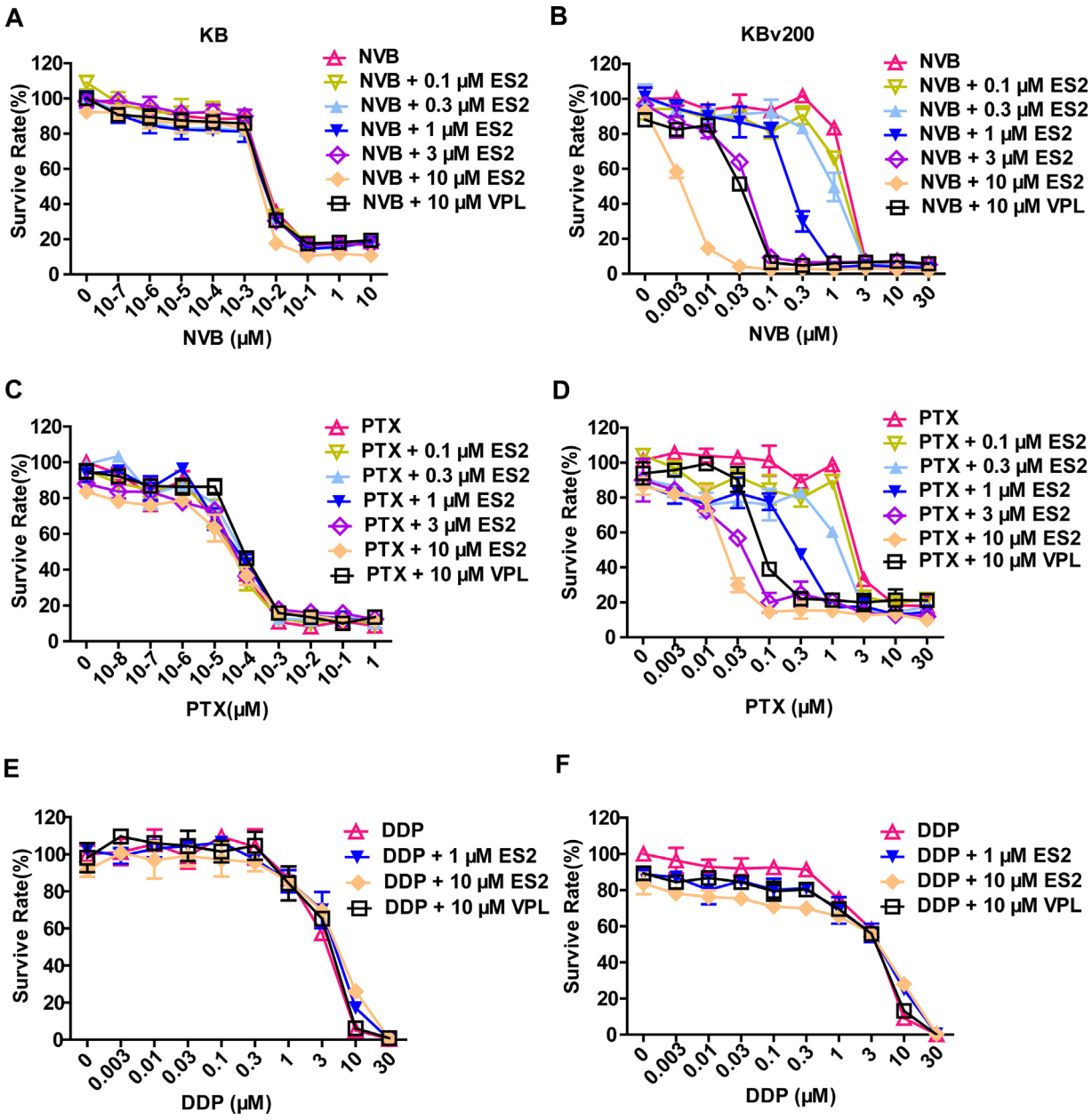

Fig. 2. ES2 enhances the sensitivity of ABCB1-substrate chemotherapeutic agents in ABCB1-overexpressing KBv200 cells. (A–F) KB and KBv200 cells were treated with different concentration of chemotherapeutic agents (NVB, PTX and DDP, respectively) in the presence of indicated concentration of ES2 for 72 h. Cell survival was measured by MTT assay. Each point represents the mean ± SD from the cells of triplicate wells. The experiments were repeated three times.

HEK293/ABCC1 to VP-16, which was almost negligible compared with its effect to reverse ABCB1-mediated drug resistance (Fig. 4C and Table 3). Together, these results demonstrated that ES2 did not reverse ABCG2- or slightly affect ABCC1-mediated MDR, but significantly overcome ABCB1-mediated MDR *in vitro*.

3.4. ES2 increases the intercellular accumulation of rhodamine 123 and doxorubicin in ABCB1-overexpressing cells

To examine whether ES2 antagonizing ABCB1-mediated cancer MDR is due to its inhibitory effect on the transporter function of ABCB1, we measured the intracellular levels of two substrates of ABCB1, rhodamine 123 (Rho123) and doxorubicin (DOX) in the presence or absence of ES2 using fluorescence microscope and flow cytometry. As shown in Fig. 5A, the intracellular levels of Rho123 and DOX in KBv200 and DOX in MCF-7/ADR were significantly lower than those in KB and MCF-7 cells, respectively. ES2 treatment induced a remarkable increase in intracellular accumulation of Rho123 and DOX in KBv200 and MCF-7/ADR cells, which were indicated by the stronger fluorescence intensities. Of note, the effect of ES2 at 10 μM on the accumulation of Rho123 and DOX obviously outperformed verapamil at the same concentration.

Then the intracellular accumulation of Rho123 and DOX were quantitated by flow cytometry. As shown in Fig. 5B, ES2 concentration-dependently increased the intracellular levels of Rho123 and DOX in KBV200 and MCF-7/ADR cells but not in KB and MCF-7 cells, respectively. This phenomenon was also observed in ES2 treated ABCB1-overexressing A549/T cells (Supplemental Fig. S2). Meaningfully, ES2 at 1 μM exhibited similar or better effect on increasing Rho123 or DOX accumulation as verapamil did at 10 μM in all three cell lines. Therefore, these results demonstrated that ES2 promoted the intracellular accumulation of ABCB1 substrates.

Please cite this article in press as: Y. Fang, et al., ES2 enhances the efficacy of chemotherapeutic agents in ABCB1-overexpressing cancer cells in vitro and in vivo, Pharmacol Res (2017), https://doi.org/10.1016/j.phrs.2017.11.001

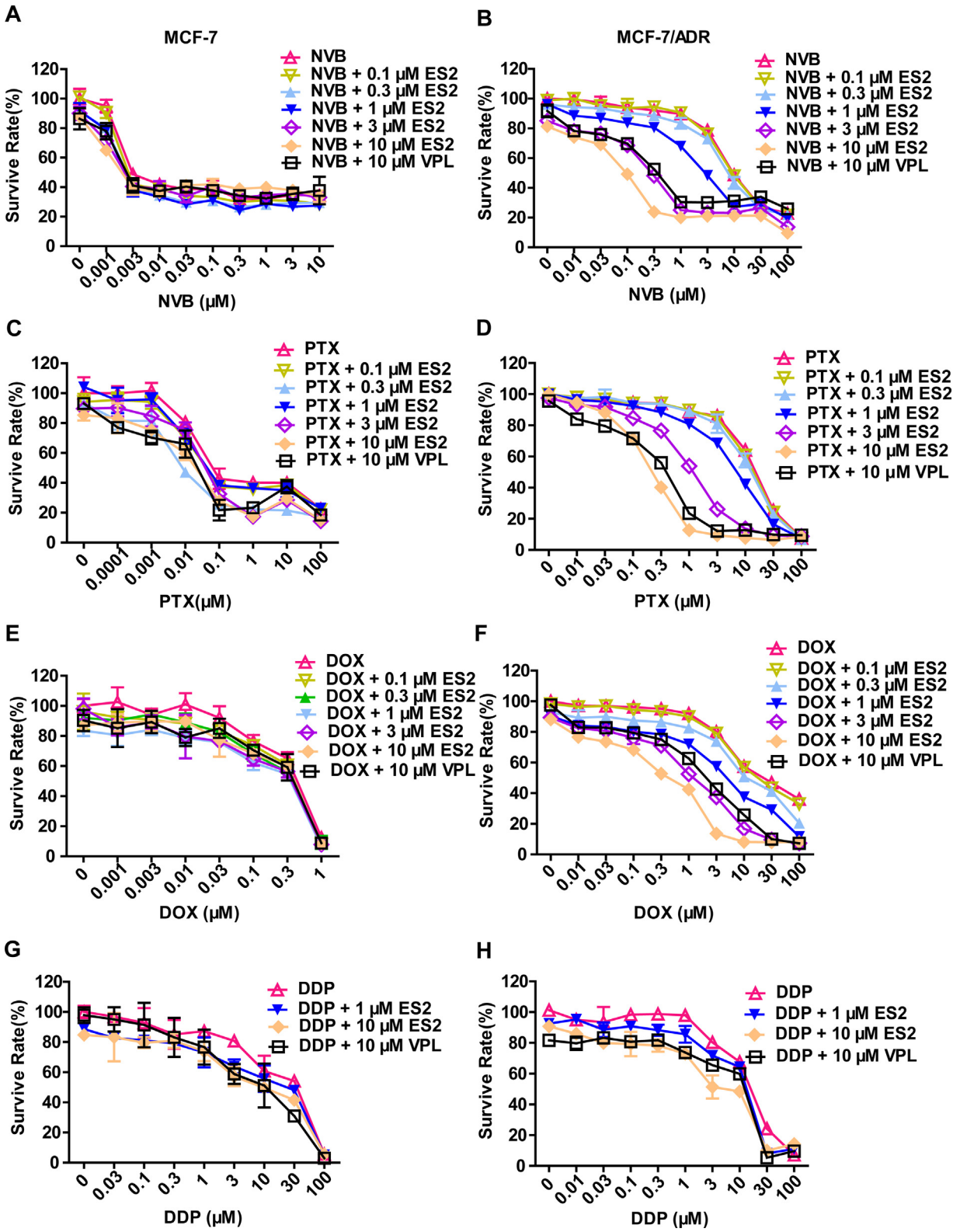

Fig. 3. ES2 enhances the sensitivity of ABCB1-substrate chemotherapeutic agents in ABCB1-overexpressing MCF-7/ADR cells. (A–H) MCF-7 and MCF-7/ADR cells were treated with different concentration of chemotherapeutic agents (NVB, PTX, DOX and DDP, respectively) in the presence of indicated concentration of ES2 for 72 h. Cell survival was measured by MTT assay. Each point represents the mean ± SD from the cells of triplicate wells. The experiments were repeated three times.

3.5. ES2 significantly decreases the efflux of Rho123 in ABCB1-overexpressing cells

To determine whether the increased intracellular accumulation of ABCB1 substrates was due to an inhibition of substrates efflux, we performed a time course study to evaluate the efflux of Rho123 in the presence of ES2 in KBv200 and its parental KB cells. As expected, KBv200 cells extruded a significantly higher percentage of accumulated Rho123 compared to KB cells. The accumulation of Rho123 at

Table 1
Effect of ES2 on reversing ABCB1-mediated MDR in KBv200 cells.

Compounds	$IC_{50} \pm SD$ (μM) (fold-reversal)			
	KB		KBv200	
NVB	0.0053 ± 0.0001	(1.00)	1.367 ± 0.136	(1.00)
+ES2 0.1 μM	0.0050 ± 0.0009	(1.06)	1.194 ± 0.097	(1.14)
+ES2 0.3 μM	0.0049 ± 0.0004	(1.09)	1.021 ± 0.100***	(1.34)
+ES2 1 μM	0.0050 ± 0.0004	(1.07)	0.224 ± 0.016***	(6.09)
+ES2 3 μM	0.0044 ± 0.0003	(1.22)	0.041 ± 0.004***	(33.69)
+ES2 10 μM	0.0035 ± 0.0005	(1.54)	0.004 ± 0.004***	(315.44)
+VPL 10 μM	0.0055 ± 0.0018	(0.97)	0.031 ± 0.001***	(43.88)
PTX	0.0073 ± 0.0005[a]	(1.00)	1.858 ± 0.640	(1.00)
+ES2 0.1 μM	0.0064 ± 0.0014[a]	(1.14)	1.606 ± 0.381	(1.16)
+ES2 0.3 μM	0.0072 ± 0.0010[a]	(1.02)	1.150 ± 0.161	(1.62)
+ES2 1 μM	0.0066 ± 0.0009[a]	(1.10)	0.295 ± 0.013**	(6.29)
+ES2 3 μM	0.0071 ± 0.0001[a]	(1.03)	0.037 ± 0.010**	(50.41)
+ES2 10 μM	0.0072 ± 0.0013[a]	(1.02)	0.023 ± 0.004**	(82.54)
+VPL 10 μM	0.0083 ± 0.0004[a]	(0.88)	0.071 ± 0.017**	(26.25)
DDP	1.481 ± 0.063	(1.00)	1.570 ± 0.089	(1.00)
+ES2 1 μM +ES2 10 μM	1.416 ± 0.1791.647 ± 0.223	(1.05)(0.90)	1.482 ± 0.1201.376 ± 0.069	(1.06)(1.14)
+VPL 10 μM	1.587 ± 0.444	(0.93)	1.686 ± 0.366	(0.93)

Drug cytotoxicity was evaluated in KB and KBv200 by MTT assay as described in the Materials and Methods. VPL was used as the positive control. Data are the mean ± SD from triplicate wells. The experiments were repeated three times and a representative data was shown. The fold-reversal of MDR (values given in parentheses) was calculated by dividing the IC_{50} for cells with the chemotherapeutic drugs in the absence of ES2 by that obtained in the presence of ES2. $^{**}P < 0.01$ and $^{***}P < 0.001$ for values *vs.* that obtained in the absence of ES2 or VPL.

[a] The unit of IC_{50} values was nM.

Table 2
Effect of ES2 on reversing ABCB1-mediated MDR in MCF-7/ADR cells.

Compounds	$IC_{50} \pm SD$ (μM) (fold-reversal)			
	MCF-7		MCF-7/ADR	
NVB	0.0065 ± 0.0001	(1.00)	11.849 ± 1.533	(1.00)
+ES2 0.1 μM	0.0058 ± 0.0007	(1.13)	13.449 ± 0.620	(0.88)
+ES2 0.3 μM	0.0044 ± 0.0001	(1.47)	11.548 ± 2.267	(1.03)
+ES2 1 μM	0.0041 ± 0.0007	(1.58)	4.431 ± 0.460***	(2.67)
+ES2 3 μM	0.0065 ± 0.0016	(1.00)	0.512 ± 0.049***	(23.12)
+ES2 10 μM	0.0053 ± 0.0012	(1.21)	0.193 ± 0.011***	(61.34)
+VPL 10 μM	0.0046 ± 0.0009	(1.42)	0.534 ± 0.101***	(22.20)
PTX	0.024 ± 0.012	(1.00)	21.747 ± 4.066	(1.00)
+ES2 0.1 μM	0.014 ± 0.003	(1.77)	28.693 ± 0.784	(0.76)
+ES2 0.3 μM	0.009 ± 0.002	(2.57)	17.167 ± 1.620*	(1.27)
+ES2 1 μM	0.014 ± 0.005	(1.66)	9.750 ± 0.553***	(2.23)
+ES2 3 μM	0.032 ± 0.006	(0.76)	0.554 ± 0.080***	(39.29)
+ES2 10 μM	0.014 ± 0.008	(1.72)	0.216 ± 0.045***	(100.82)
+VPL 10 μM	0.028 ± 0.029	(0.84)	0.873 ± 0.112***	(24.90)
DOX	0.245 ± 0.0003	(1.00)	27.984 ± 1.422	(1.00)
+ES2 0.1 μM	0.317 ± 0.003	(0.77)	25.326 ± 2.419	(1.10)
+ES2 0.3 μM	0.241 ± 0.071	(1.02)	17.798 ± 1.326***	(1.57)
+ES2 1 μM	0.248 ± 0.069	(0.99)	6.780 ± 0.476***	(4.13)
+ES2 3 μM	0.245 ± 0.057	(1.00)	1.574 ± 0.285***	(17.78)
+ES2 10 μM	0.319 ± 0.003	(0.77)	0.455 ± 0.045***	(61.48)
+VPL 10 μM	0.314 ± 0.011	(0.78)	1.653 ± 0.190***	(16.93)
DDP	11.698 ± 4.606	(1.00)	15.576 ± 0.460	(1.00)
+ES2 1 μM	7.117 ± 1.208	(1.64)	10.893 ± 0.146	(1.43)
+ES2 10 μM	7.162 ± 1.316	(1.63)	7.444 ± 0.342	(2.09)
+VPL 10 μM	6.920 ± 1.153	(1.69)	10.923 ± 0.135	(1.43)

Drug cytotoxicity was evaluated in MCF-7 and MCF-7/ADR by MTT assay as described in the Materials and Methods. VPL was used as the positive control. Data are the mean ± SD from triplicate wells. The experiments were repeated three times and a representative data was shown. The fold-reversal of MDR (values given in parentheses) was calculated by dividing the IC_{50} for cells with the chemotherapeutic drugs in the absence of ES2 by that obtained in the presence of ES2. $^{*}P < 0.05$, $^{**}P < 0.01$ and $^{***}P < 0.001$ for values *vs.* that obtained in the absence of ES2 or VPL.

0 min was set at 100% and at 15, 30, 60, 90 and 120 min, the percentages of the remaining Rho123 in KBv200 cells were 35.92%, 13.68%, 6.16%, 3.76% and 6.03%, respectively. With the addition of ES2, the percentages of the remaining Rho123 in KBv200 cells increased to 103.93%, 68.50%, 42.88%, 45.82% and 25.08%, respectively (Fig. 5C). However, ES2 did not influence drug efflux in sensitive KB cells. Collectively, these results suggested that ES2 was able to modulate MDR by attenuating the efflux of ABCB1 substrates, thereby increasing their intracellular accumulation.

3.6. ES2 stimulates the ATPase activity of ABCB1

ABCB1 is an ATP-dependent membrane transporter, and its drug-efflux function depends on the ATP hydrolysis, which is stimulated when ABCB1 interacts with its modulators [23,24]. To assess the effect of ES2 on the ATPase activity of ABCB1, we tested the ABCB1-mediated ATP hydrolysis after treated with different concentrations of ES2 (0–50 μM). As illustrated in Fig. 6A, ES2 enhanced ABCB1 ATPase activity in a concentration-dependent manner with a maximal stimulation of 4.7-fold of the basal activity.

Please cite this article in press as: Y. Fang, et al., ES2 enhances the efficacy of chemotherapeutic agents in ABCB1-overexpressing cancer cells *in vitro* and *in vivo*, Pharmacol Res (2017), https://doi.org/10.1016/j.phrs.2017.11.001

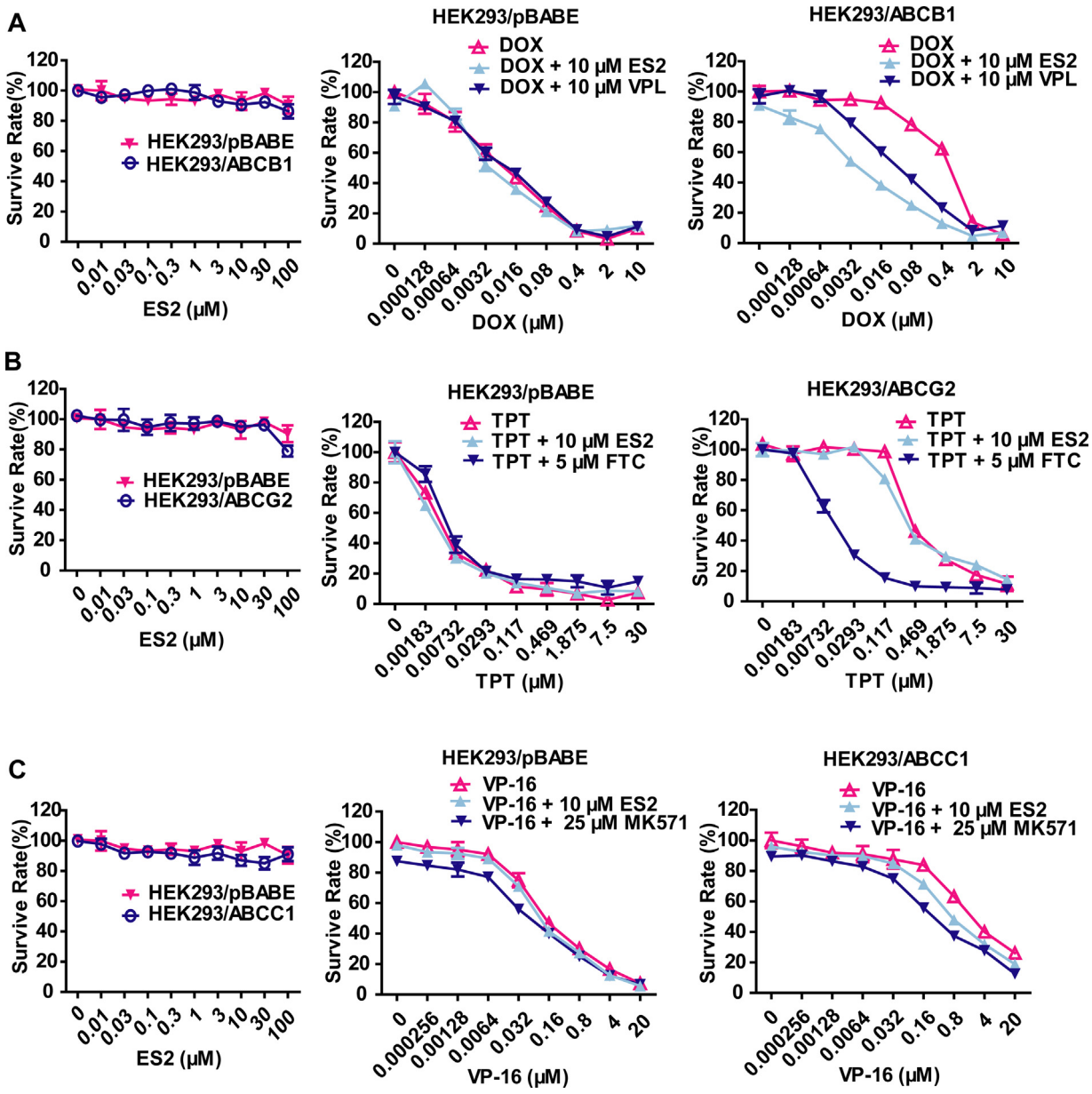

Fig. 4. ES2 does not enhance the sensibility of ABCG2- or ABCC1-overexpressing cells to chemotherapeutic agents. Cells were treated with ES2 alone or in combination with different concentration of chemotherapeutic agents (DOX, TPT and VP-16, respectively) for 72 h. Cell survival was measured by MTT assay. Each point represents the mean ± SD from the cells of triplicate wells. The experiments were repeated three times.

We then examined the effect of ES2 on verapamil-stimulated ABCB1 ATPase activity. As shown in Fig. 6B, ES2 had no impact on verapamil-stimulated ABCB1 ATPase activity.

Given that the reversal of ABCB1-mediated MDR can be achieved either by inhibiting its pump activity or by decreasing its expression [10], we then determined the mRNA and protein levels of ABCB1 in KBv200 and MCF-7/ADR cells after ES2 treatment. The results showed that neither the mRNA nor the protein level of ABCB1 was altered in KBv200 and MCF-7/ADR cells treated with different concentration of ES2 or with different times even up to 72 h (Fig. 6C and D). Together, these results demonstrated that ES2 could stimulate the ATPase activity of ABCB1, but did not affect the expression of ABCB1, suggesting that ES2 might be a substrate of ABCB1.

3.7. Model for binding of ES2 to ABCB1

To better understand the interaction between compound ES2 and ABCB1, we performed a virtual docking experiment. Docking simulation of ES2 into the binding site of ABCB1 (PDB ID: 4M2S) had better scoring pose (-7.2) and was chosen for analysis of ES2-ABCB1 binding interactions. As shown in Fig. 7, ES2 (labeled in yellow) could fit into the drug-binding cavity of human homology ABCB1 as VPL (labeled in green) did. Interestingly, ES2 shared some binding sites with verapamil, including the residues GLN979, MET975, PHE972, GLN714, ALA976, ILE329, LEU328, PHE325, PHE717 and TYR299. But the binding sites of ES2 and verapamil to ABCB1 were not completely overlapped. ES2 was also found to interact with residues GLN336, GLY335, THR188, LEU57, PHE332 and SER982. This docking result further confirmed ES2-induced ABCB1 malfunction may through directly binding to it.

3.8. ES2 potentiates the anticancer activity of NVB in ABCB1-overexpressing tumor xenograft nude mouse model

KBv200 cell xenograft model in nude mice was used to investigate the efficacy of ES2 to reverse resistance to NVB *in vivo*. There

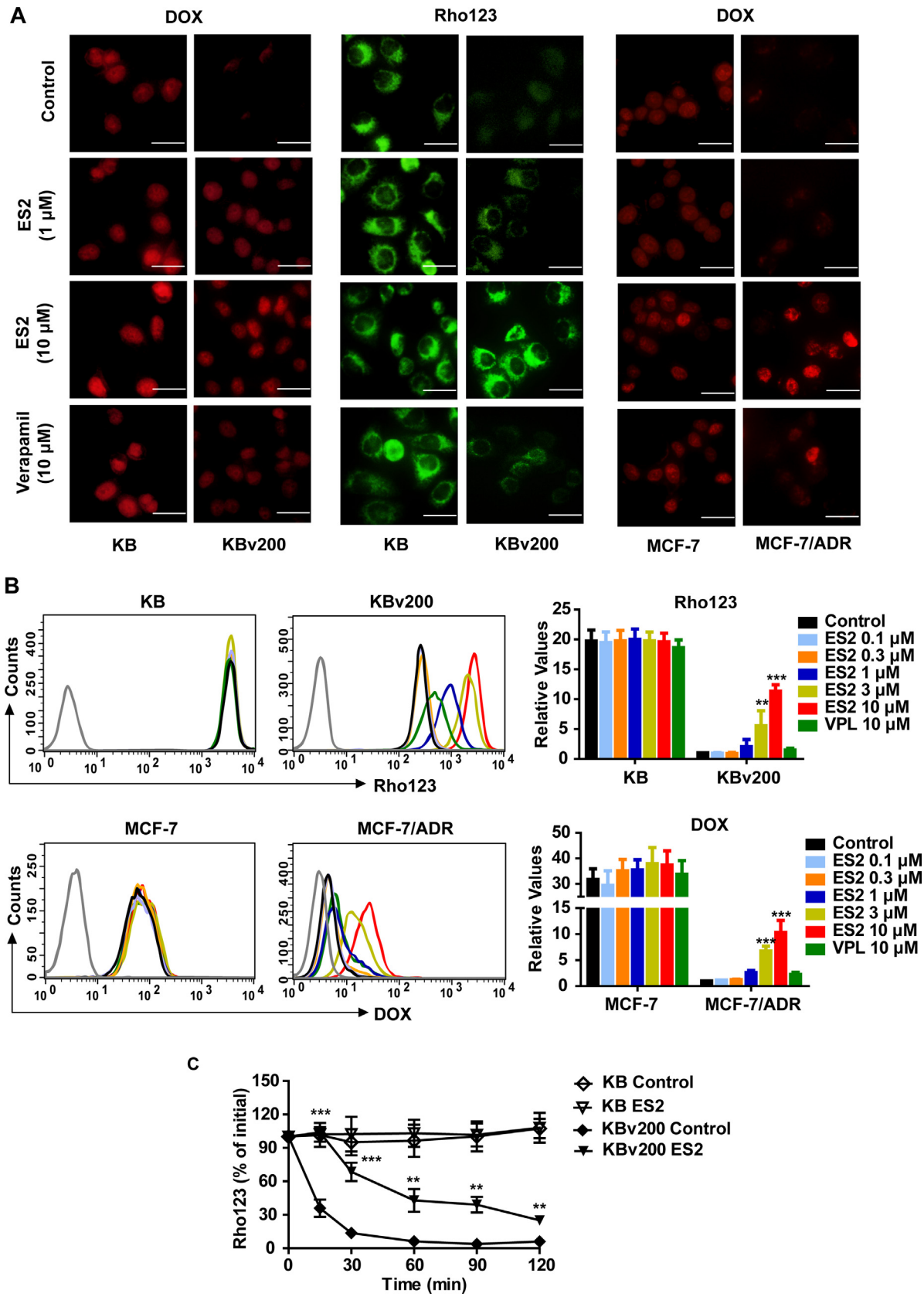

Fig. 5. ES2 increases intracellular accumulation of DOX and/or Rho123 and decreases efflux of Rho123. (A) Fluorescence microscopy observation of the intracellular accumulation of DOX and/or Rho123 in KB, KBv200, MCF-7 and MCF-7/ADR cells. The results are representative images of three independent experiments. Scale bar, 20 μm. (B) The accumulation of Rho123 in KB and KBv200 cells and DOX in MCF-7 and MCF-7/ADR cells were measured by flow cytometric analysis. The data are presented as fold-change in fluorescence intensity relative to control cells (KBv200 or MCF-7/ADR). (C) Time course of Rho123 efflux was measured in KB and KBv200 cells in the presence or absence of ES2 (10 μM). The results are shown as the mean ± SD of three independent experiments. $^{***}P < 001$, $^{**}P < 0.01$ *vs.* vehicle-treated KBv200 cells.

Please cite this article in press as: Y. Fang, et al., ES2 enhances the efficacy of chemotherapeutic agents in ABCB1-overexpressing cancer cells *in vitro* and *in vivo*, Pharmacol Res (2017), https://doi.org/10.1016/j.phrs.2017.11.001

Table 3
Effect of ES2 on reversing ABCB1-, ABCG2- and ABCC1-mediated MDR in stable-transfected cells.

Compounds	$IC_{50} \pm SD$ (μM) (fold-reversal)			
	HEK293/pBABE		HEK293/ABCB1	
DOX	0.009 ± 0.005	(1.00)	0.328 ± 0.059	(1.00)
+ES2 10 μM	0.006 ± 0.004	(1.50)	0.005 ± 0.001***	(65.6)
+VPL 10 μM	0.010 ± 0.010	(0.90)	0.031 ± 0.023**	(10.58)
Compounds	$IC_{50} \pm SD$ (μM) (fold-reversal)			
	HEK293/pBABE		HEK293/ABCG2	
TPT	0.007 ± 0.001	(1.00)	0.870 ± 0.095	(1.00)
+ES2 10 μM	0.004 ± 0.001	(1.75)	0.575 ± 0.119	(1.51)
+FTC 5 μM	0.008 ± 0.002	(0.88)	0.018 ± 0.005**	(43.45)
Compounds	$IC_{50} \pm SD$ (μM) (fold-reversal)			
	HEK293/pBABE		HEK293/ABCC1	
VP-16	0.100 ± 0.055	(1.00)	2.844 ± 0.556	(1.00)
+ES2 10 μM	0.074 ± 0.048	(1.35)	1.084 ± 0.395*	(2.63)
+MK571 25 μM	0.050 ± 0.025	(2.00)	0.381 ± 0.191**	(7.47)

Drug cytotoxicity was evaluated by MTT assay as described in the Materials and Methods. VPL (specific inhibitor of ABCB1), FTC (specific inhibitor of ABCG2) and MK571 (specific inhibitor of ABCC1) were used as the positive control. Data are the mean ± SD from triplicate wells. The experiments were repeated three times and a representative data was shown. The fold-reversal of MDR (values given in parentheses) was calculated by dividing the IC_{50} for cells with the chemotherapeutic drugs in the absence of inhibitor by that obtained in the presence of inhibitor. *$P < 0.05$, **$P < 0.01$ and ***$P < 0.001$ for values *vs.* that obtained in the absence of inhibitor.

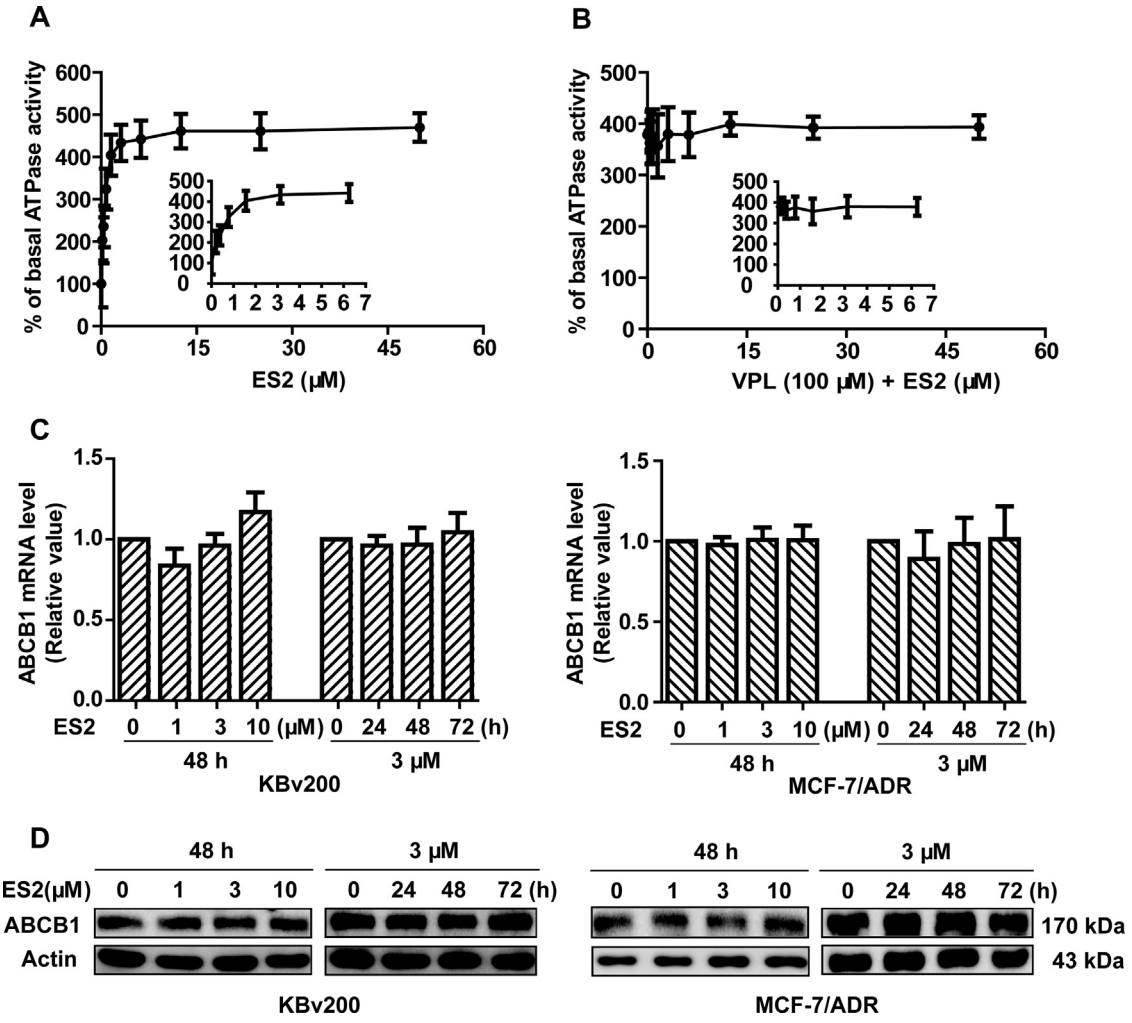

Fig. 6. ES2 stimulates the ATPase activity of ABCB1 and did not affect the expression of ABCB1. (A) The ABCB1 ATPase activity were determined after incubated with increasing concentrations of ES2 (0–50 μM). (B) The ABCB1 ATPase activity were determined after incubated with increasing concentrations of ES2 (0–50 μM) in the presence of VPL (100 μM). (C) The mRNA expression of ABCB1 in KBv200 cells was determined by real-time PCR. The results are shown as the mean ± SD of three independent experiments. (D) The protein expression of ABCB1 in KBv200 cells was determined by western blot analysis. The results are representative of three independent experiments.

Please cite this article in press as: Y. Fang, et al., ES2 enhances the efficacy of chemotherapeutic agents in ABCB1-overexpressing cancer cells *in vitro* and *in vivo*, Pharmacol Res (2017), https://doi.org/10.1016/j.phrs.2017.11.001

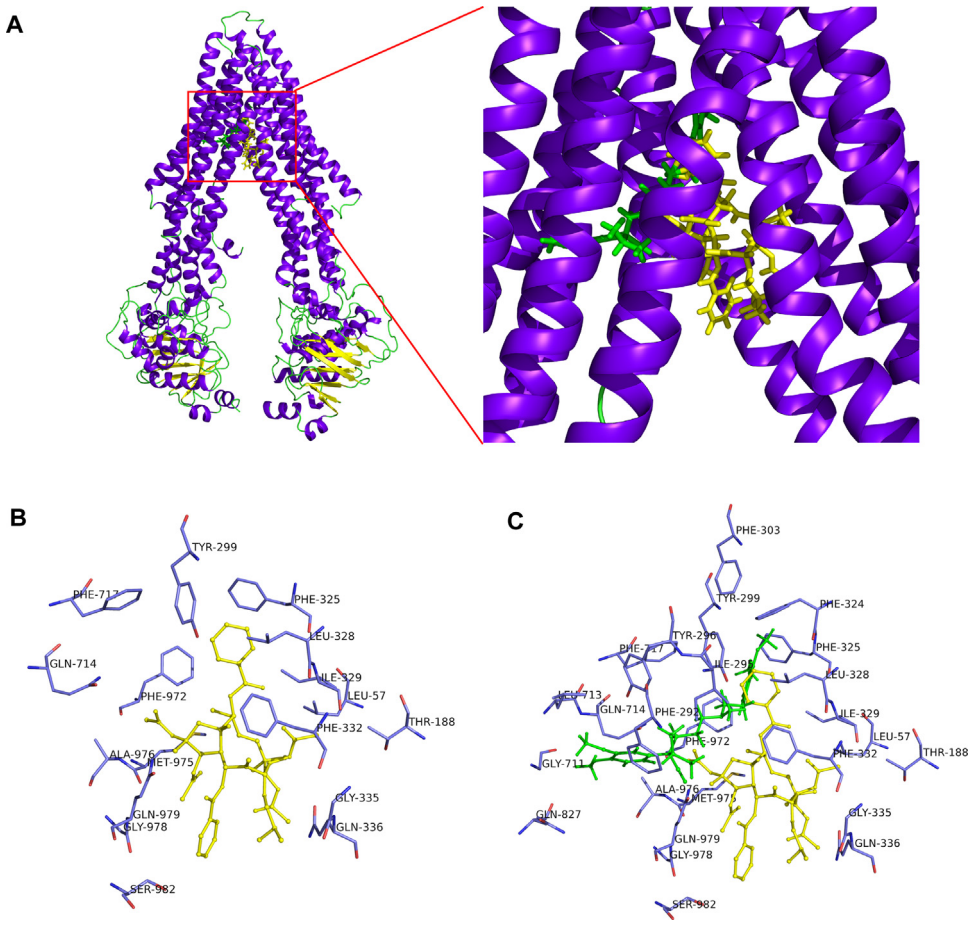

Fig. 7. Docking analysis of ES2 and VPL toward ABCB1. (A) The binding mode and position of ES2 and VPL with ABCB1. (B) The residual amino acid around ES2. (C) The residual amino acid around ES2 and VPL.

was no significant difference in tumor size among animals treated with vehicle, NVB, and ES2 alone. But the combination of ES2 and NVB significantly inhibited tumor growth compared with vehicle, NVB or ES2, and the TGI% was 43% (Fig. 8A and B). Moreover, the average tumor weight of ES2 and NVB-treated mice was significantly lower than that of saline-treated mice (Fig. 8C). In addition, there was no animal death or obvious body weight loss in all these four groups (Fig. 8D). These results indicated that ES2 had a significant reversal effect on ABCB1-mediated MDR *in vivo* and did not lead to increased side effects.

4. Discussion

Given the properties of low toxicity and few side effects, active constituents from natural plants to reverse MDR have attracted plenty of interest. We have previously isolated a new type of Jatrophane diterpenoid ester, ES2 from the fructus E. *sororia* and found it increased the intracellular accumulation of Rho123 in ABCB1-overexpessing cells [15]. In this paper, we determined the effect of ES2 on reversing ABCB1-mediated MDR *in vitro* and *in vivo*, and investigated the mechanisms by which ES2 exerts its MDR reversal activity.

The anti-proliferative activity of ES2 on ABCB1-overexpressing cells (KBv200, MCF-7/ADR and A549/T) and their parental cells (KB, MCF-7 and A549) were very weak, as more than 85% of cancer cells remained survival after treated with ES2 for 72 h at 10 μM. The MDR reversal activity of ES2 could be detected at concentration as low as 0.3 μM. ES2 at non-cytotoxic concentrations (0.3–10 μM) significantly increased the sensitivity of KBv200 and MCF-7/ADR to NVB, PTX and DOX which are substrates of ABCB1, whereas it could not appreciably affect the cytotoxicity of these drugs in the parental sensitive KB and MCF-7 cells. Of note, the ability of ES2 at 10 μM to decrease the IC_{50} values of these chemotherapeutic agents was much better than that of VPL at the same concentration. Moreover, ES2 did not affect the cytotoxicity of DDP, which is not a substrate of ABCB1, in both resistant and parental cells. ES2 did not reverse ABCG2- or slightly affect ABCC1-mediated MDR. These results demonstrated ES2 can increase the sensitivity of ABCB1-mediated MDR cells to chemotherapeutic agents.

To demonstrate the mechanism of the reversal effect of ES2, we investigated whether ES2 could inhibit the efflux function of ABCB1 to enhance the cytotoxicity of agents by increasing the intracellular drug concentration. It was found ES2 significantly enhanced the intracellular accumulation of Rho123 and DOX in drug resistant cells. Moreover, ES2 remarkably reduced the efflux ratio of Rho123 in drug resistant cells. These findings suggested that ES2 sensitized ABCB1-overexpressing cells to chemotherapeutic agents by inhibiting the efflux function of ABCB1 transporter, thus increasing the intracellular accumulation of chemotherapeutic agents which exerted anti-proliferative effects on drug resistant cells.

The drug-efflux function of ABCB1 is known to utilize energy from ATP hydrolysis, so the rate of ATP hydrolysis is directly proportional to the transport activity of ABCB1 [23,24]. We found that ES2 stimulated ABCB1 ATPase activity in a concentration-dependent manner and ES2 had no inhibitory effect on VPL stimulated ATPase activity, suggesting ES2 might have direct interaction with ABCB1, which may be different from VPL. Docking simulation study was further conducted with human ABCB1 homology model to illustrate

Please cite this article in press as: Y. Fang, et al., ES2 enhances the efficacy of chemotherapeutic agents in ABCB1-overexpressing cancer cells *in vitro* and *in vivo*, Pharmacol Res (2017), https://doi.org/10.1016/j.phrs.2017.11.001

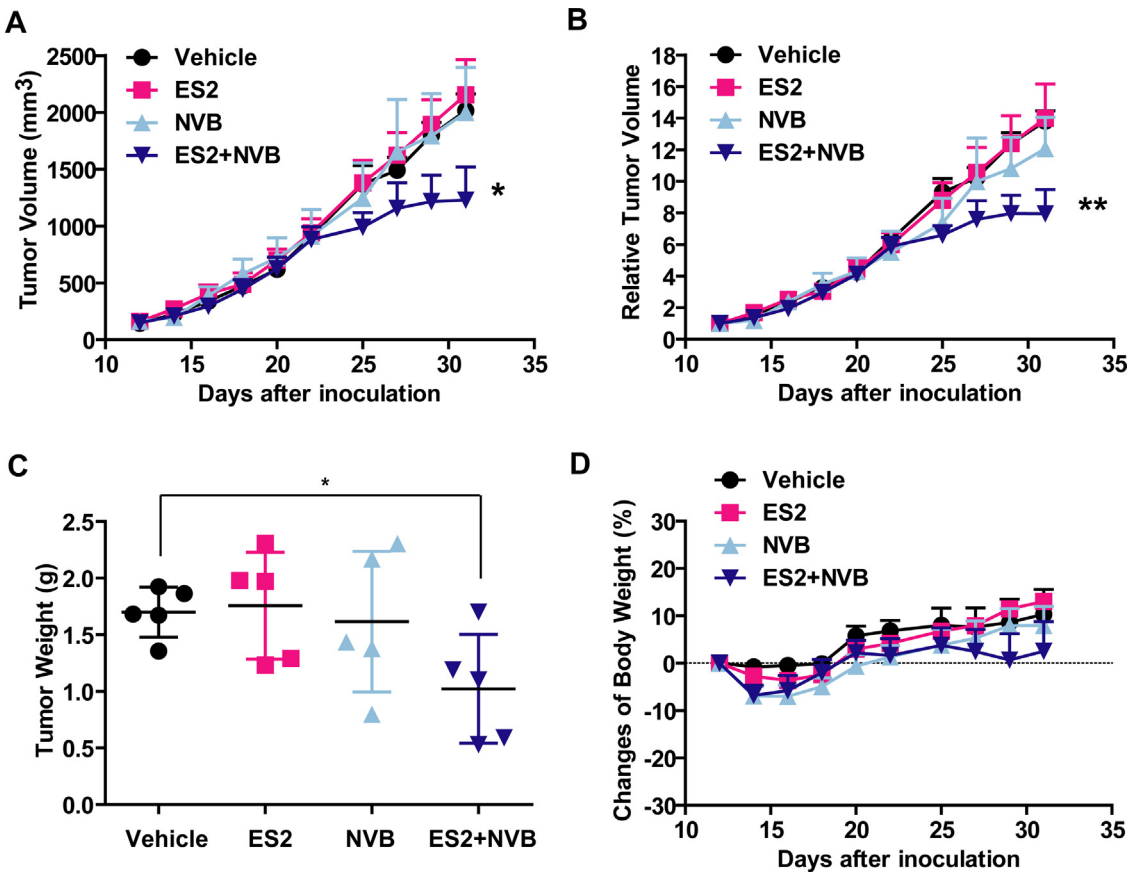

Fig. 8. ES2 in combination with NVB inhibits the growth of KBV200 xenografts in nude mice. (A) The tumor volume and (B) Relative tumor volume were plotted against days post inoculation. (C) Tumor weights. (D) Changes of body weight of mice. Data presented are the mean ± SD (n = 5). $^{*}P < 0.05$, $^{**}P < 0.01$ *vs.* vehicle-treated mice.

the molecular interaction between ES2 and ABCB1. The docking results pointed out that ES2 binding to ABCB1 partly coincided with the sites of verapamil, but did not completely overlap. Together, ES2 might work as a substrate of ABCB1 to reverse the MDR of ABCB1-overexpressing cells to chemotherapeutic agents.

The decreased ABCB1 transporting function can also be resulted from the downregulation of ABCB1 expression [10]. However, the real-time PCR and Western blot analysis of ABCB1 expression showed that neither mRNA nor protein level of ABCB1 was altered by ES2 in KBv200 and MCF-7/ADR cells. These findings support that ES2 suppressed the efflux function of ABCB1 by a mechanism other than downregulating the expression of ABCB1.

In conclusion, our results showed that ES2, a new type of Jatrophane diterpenoid ester, reversed ABCB1-mediated MDR by inhibition of its drug efflux function, and increased the intracellular accumulation of chemotherapeutic agents in ABCB1-overexpressing cells. We further found the MDR reversal effect of ES2 might be related with its binding to ABCB1 as a substrate, which was supported by its ability to stimulate the ATPase activity and the binding mode predicted by docking analysis. In addition, ES2 had no effect on downregulating the protein level of ABCB1. These findings provided solid evidence in supporting the application of ES2 in combination with chemotherapeutic agents for cancer treatment.

Conflict of interest

The authors declare that they have no conflict of interest.

Acknowledgments

This work was supported by funds from the National Natural Science Foundation of China (No. 21572263, 81373964 and 81402953), Shanghai Science & Technology Innovation Action program (No. 15140904800 and 14431902700), the National Science & technology Major Project of China (2014ZX09301-306-03), and China Postdoctoral Science Foundation (2015T80416).

Appendix A. Supplementary data

Supplementary data associated with this article can be found, in the online version, at https://doi.org/10.1016/j.phrs.2017.11.001.

References

[1] G. Szakacs, et al., Targeting multidrug resistance in cancer, Nat. Rev. Drug Discov. 5 (3) (2006) 219–234.
[2] H. Cui, et al., ABC transporter inhibitors in reversing multidrug resistance to chemotherapy, Curr. Drug Targets 16 (12) (2015) 1356–1371.
[3] W. Li, et al., Overcoming ABC transporter-mediated multidrug resistance: molecular mechanisms and novel therapeutic drug strategies, Drug Resist. Update 27 (2016) 14–29.
[4] Z. Chen, et al., Mammalian drug efflux transporters of the ATP binding cassette (ABC) family in multidrug resistance: a review of the past decade, Cancer Lett. 370 (1) (2016) 153–164.
[5] V. Vauthier, C. Housset, T. Falguieres, Targeted pharmacotherapies for defective ABC transporters, Biochem. Pharmacol. 136 (2017) 1–11.
[6] S.G. Aller, et al., Structure of P-glycoprotein reveals a molecular basis for poly-specific drug binding, Science 323 (5922) (2009) 1718–1722.
[7] F.J. Sharom, The P-glycoprotein multidrug transporter, Essays Biochem. 50 (1) (2011) 161–178.
[8] E.E. Chufan, H.M. Sim, S.V. Ambudkar, Molecular basis of the polyspecificity of P-glycoprotein (ABCB1): recent biochemical and structural studies, Adv. Cancer Res. 125 (2015) 71–96.
[9] R. Badhan, J. Penny, In silico modelling of the interaction of flavonoids with human P-glycoprotein nucleotide-binding domain, Eur. J. Med. Chem. 41 (3) (2006) 285–295.
[10] N. Wei, et al., H1: a novel derivative of tetrandrine reverse P-glycoprotein-mediated multidrug resistance by inhibiting transport

function and expression of P-glycoprotein, Cancer Chemother. Pharmacol. 67 (5) (2011) 1017–1025.
[11] J. Li, et al., Emodin sensitizes paclitaxel-resistant human ovarian cancer cells to paclitaxel-induced apoptosis *in vitro*, Oncol. Rep. 21 (6) (2009) 1605–1610.
[12] J. Yu, et al., Advances in plant-based inhibitors of P-glycoprotein, J. Enzyme Inhib. Med. Chem. 31 (6) (2016) 867–881.
[13] Y. Huang, H.A. Aisa, Jatrophane diterpenoids from fructus euphorbia sororia, Phytochem. Lett. 3 (4) (2010) 176–180.
[14] Y. Huang, H.A. Aisa, Three new diterpenoids from *Euphorbia sororia* L, Helv. Chim. Acta 93 (6) (2010) 1156–1161.
[15] D. Lu, Y. Liu, H.A. Aisa, Jatrophane diterpenoid esters from *Euphorbia sororia* serving as multidrug resistance reversal agents, Fitoterapia 92 (2014) 244–251.
[16] C.K. Firempong, et al., Segetoside I, a plant-derived bisdesmosidic saponin, induces apoptosis in human hepatoma cells *in vitro* and inhibits tumor growth *in vivo*, Pharmacol. Res. 110 (2016) 101–110.
[17] D. Qiao, et al., UMMS-4 enhanced sensitivity of chemotherapeutic agents to ABCB1-overexpressing cells via inhibiting function of ABCB1 transporter, Am. J. Cancer. Res. 4 (2) (2014) 148–160.
[18] D.M. Zhang, et al., BBA: a derivative of 23-hydroxybetulinic acid, potently reverses ABCB1-mediated drug resistance *in vitro* and *in vivo*, Mol. Pharm. 9 (11) (2012) 3147–3159.
[19] X.Q. Zhao, et al., Neratinib reverses ATP-binding cassette B1-mediated chemotherapeutic drug resistance *in vitro*, *in vivo*, and *ex vivo*, Mol. Pharmacol. 82 (1) (2012) 47–58.
[20] Z. Li, et al., Glucocorticoid up-regulates transforming growth factor-beta (TGF-beta) type II receptor and enhances TGF-beta signaling in human prostate cancer PC-3 cells, Endocrinology 147 (11) (2006) 5259–5267.
[21] Y.J. Wang, et al., Motesanib (AMG706): a potent multikinase inhibitor, antagonizes multidrug resistance by inhibiting the efflux activity of the ABCB1, Biochem. Pharmacol. 90 (4) (2014) 367–378.
[22] R. Roskoski Jr., Guidelines for preparing color figures for everyone including the colorblind, Pharmacol. Res. 119 (2017) 240–241.
[23] B. Verhalen, et al., Energy transduction and alternating access of the mammalian ABC transporter P-glycoprotein, Nature (2017).
[24] E.E. Chufan, K. Kapoor, S.V. Ambudkar, Drug-protein hydrogen bonds govern the inhibition of the ATP hydrolysis of the multidrug transporter P-glycoprotein, Biochem. Pharmacol. 101 (2016) 40–53.

Please cite this article in press as: Y. Fang, et al., ES2 enhances the efficacy of chemotherapeutic agents in ABCB1-overexpressing cancer cells *in vitro* and *in vivo*, Pharmacol Res (2017), https://doi.org/10.1016/j.phrs.2017.11.001